ELSEVIER

Journal of Power Sources 107 (2002) 90–97

JOURNAL OF POWER SOURCES

www.elsevier.com/locate/jpowsour

Electrochemical characteristics of graphite coated with tin-oxide and copper by fluidised-bed chemical vapour deposition

Joong Kee Lee[a,*], D.H. Ryu[b], Jeh Beck Ju[c], Y.G. Shul[b], B.W. Cho[a], D. Park[a]

[a]*Eco Nano Research Centre, Korea Institute of Science and Technology, P.O. Box 131, Cheongryang, Seoul 130-650, Korea*
[b]*Department of Chemical Engineering, Younsei University, Seoul, Korea*
[c]*Department of Chemical Engineering, Hong-Ik University, Seoul, Korea*

Received 2 July 2001; accepted 26 October 2001

Abstract

Anodes for a lithium secondary battery are prepared with synthetic graphite (meso-phase carbonaceous microbead: MCMB) which is coated with tin-oxide and copper by fluidised-bed chemical vapour deposition (FCVD). In the present study, three different samples was prepared, and their electrochemical characteristics are examined by using X-ray diffraction, electrochemical voltage spectroscopy (EVS), scanning electron micrography, ac impedance measurements, and galvanostatic charge–discharge experiments. The electrode coated with tin-oxide gives higher capacity than uncoated MCMB, but the capacity decreases with cycling. This is probably due to severe volume changes. The cycleability is improved, however, by coating copper on the surface of the carbonaceous material coated with tin-oxide. The copper plays an important role as an inactive matrix which provides a buffer against volume changes.

Keywords: Lithium secondary batteries; Synthetic graphite (MCMB); Tin-oxide; Copper coating; Fluidised-bed; Chemical vapour deposition

1. Introduction

Lithium intercalated carbons are employed as an anode for present commercial lithium secondary batteries. There is, however, strong interest interest in modifying the surface of active carbonaceous materials because this determines the irreversible capacity, charge–discharge capacity and high-rate capability.

The surface modification of lithiated carbon electrodes is an important factor in obtaining the proper formation of the passivation layer. Even minor variations in the composition of these surface films give rise to drastic changes in the macroscopic behaviour of the carbon anode [1]. Metals such as Ag, Pb, Al and Sn, used for the anode, have been studied for specific weight capacity. The metal electrodes show poor cycleability on account of deterioration of the electric constant or grains due to a large volume change of the metal crystals during charge–discharge cycles [2,3]. Recently, in order to overcome the problems in using metal anodes, metal–carbon composites have been tried. Replacement of carbon with an ultra-fine metal–graphite composite offers better electrochemical performance. For example, after suspending graphite powder in a water–ethanol mixture solution, highly dispersed silver metal–carbon composite can be obtained by chemical reduction reaction between Ag^+ ions and reducing agents such as HCHO or N_2H_4. The metal on the carbon surface acts as an electronic conductor as well as lithium intercalation sites to form Li–Ag alloy [4–6].

The sol–gel method has been employed to disperse tin-oxide on the surface of graphite particles and then the tin-oxide-coated graphite as an anode was used to alter the composition of the surface film on the graphite. The tin-oxide-coated graphite electrode showed better cycle performance and discharge capacity compared with an untreated graphite electrode [7,8].

To develop an alternative anode material, the effects of coating a synthetic graphite surface with tin-oxide and copper are examined in this paper. In the graphite–metallic system, it is expect that the graphite matrix will act as a lithium intercalation site and the metallic compounds on the carbon surface will form an artificial passivation film or an electronic conducting agent in the electrode. The coating was performed by chemical vapour deposition in a fluidised-bed.

2. Experimental

Commercial synthetic graphite with an average particle diameter of about 10 μm (MCMB1028, Osaka gas) was used

* Corresponding author. Tel.: +82-2-958-5252; fax: +82-2-958-5269.
E-mail address: leejk@kist.re.kr (J.K. Lee).

0378-7753/02/$ – see front matter
PII: S0378-7753(01)00985-5

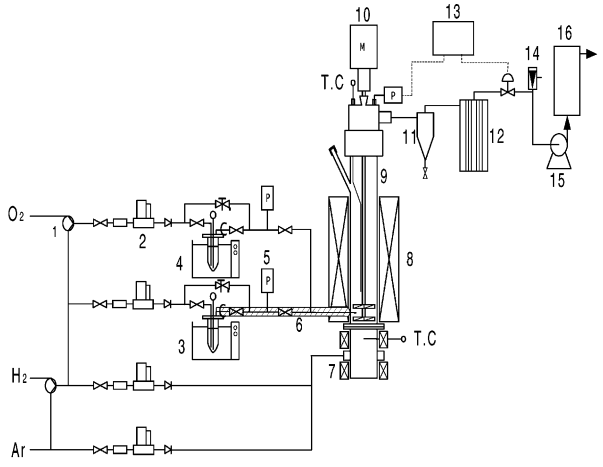

Fig. 1. Schematic diagram of fluidized-bed chemical vapour deposition process ((1) three-way valve, (2) mass flow controller, (3) bath 1 (Cu source), (4) bath 2 (Sn source), (5) pressure gauge, (6) line heater, (7) pre-heater, (8) heater, (9) reactor, (10) stirrer, (11) cyclone, (12) filter, (13) pressure controller, (14) angle valve, (15) vacuum pump, (16) exhaust gas treatment system).

as raw material. Metal–graphite composite was prepared by a fluidised-bed chemical vapour deposition (FCVD) method which used the system shown schematically in Fig. 1. The fluidised-bed reactor; comprises a quartz tube with an inside diameter of 56 mm and a length of 370 mm. The reactor was heated by an electrical heater and contained a K-type thermocouple $Cu(hfac)_2$ and $(CH_3)_4Sn$ were employed as organometallic precursors. Hydrogen or argon was used as a carrier gas to transport the precursors to the reactor. The feed rates of the precursors were controlled by adjusting the bubbler temperatures and the flow rates of the carrier gases. An impeller was positioned along the axis of the reactor to assist the mixing of the graphite particles. A sintered metal with an average pore diameter of 40 μm was used as a gas distributor. All of the gases were fed to the reactor through mass-flow controllers. The working pressure of the reactor was regulated through a control loop which consisted of a pressure gauge, a throttling valve in the gas exhaust, and a vacuum pump. In the present work, the pressure of process chamber was maintained at 740 Torr. Three different kinds of sample were prepared by FCVD. The compositions of the samples and the preparation conditions for FCVD are summarised in Table 1.

The electrodes for half-cells of lithium-ion batteries were manufactured with the above samples prepared in different conditions and their electrochemical properties were compared. The negative electrodes were fabricated by mixing a slurry which contained 6 wt.% polyvinylidene fluoride (PVdF) binder, 3 wt.% acetylene black as the conductor, and 91 wt.% active materials. The metal-coated carbon electrode did not contain the conductor. The graphite was mixed in the presence of some acetone solution in a vortex mixer at 5000 rpm. A slurry containing carbonaceous material was spread to form a 100 μm thick sheet on copper foil by the dipping method. The sheet was allowed to dry at ambient temperature for a day, followed by drying in an oven at 80 °C. The composite was then pressed at 110–120 °C by using a roll press. The pressed composite was cut into 2 cm × 2 cm pieces and dried in a vacuum at 110 °C for 24 h. All cells were assembled in a dry-room (maximum moisture $< 5\%$). The counter electrodes were lithium metal foils of 75 μm thickness and the separator was a polypropylene-based film. The electrolyte employed in this study was 1 M $LiPF_6$ dissolved in a mixture of ethylene carbonate (EC), diethyl carbonate (DEC), propylene carbonate (PC), and dimethyl carbonate (DMC).

Metal-coated graphites, prepared by the FCVD method, were characterised by inductively coupled plasma (ICP; Ash Thermo Jarrel POLYSCAN 61E), X-ray diffractometry (XRD; RIGAKU RINT/DMAS-2500) with a Cu Kα source, scanning electron microscopy (SEM; Hitachi S-4200), and electron probe micro analysis (EPMA; JEOL JXA-8600).

Typical charge–discharge cycling tests for the metal-coated graphites were carried out using galvanostatic cycling (Won A Tech WBC3000) at various rates between 0 and 1.2 V versus Li/Li^+. The ac impedance measurements for the metal-coated graphites were performed under open-circuit conditions in a frequency range from 0.1 to 10^6 Hz. The perturbation amplitude was ±5 mV. The employed experimental set-up consisted of a frequency response analyser and a potentiostat/galvanostat (ZAHNER JM6) [9]. For electrochemical voltage spectroscopy (EVS) experiment, a series of constant potential steps were applied to the cells prepared by FCVD and raw MCMB. The charge

Table 1
Deposition conditions for FCVD

No.	Elemental analysis[a]		FCVD reaction conditions
	Cu (wt.%)	Sn (wt.%)	
S0[b]	–	–	–
S1	–	1.37	Tin-oxide coating at ∼500 °C for 30 min
S2	–	0.93	Tin-oxide coating at ∼500 °C for 10 min
S3	0.14	1.83	Tin-oxide coating at ∼500 °C for 40 min, and subsequently copper coating at ∼400 °C for 1 h

[a] Determined by ICP.
[b] Raw MCMB.

accumulated in each potential step was integrated to yield a dQ/dV versus V plot.

3. Results and discussion

As shown in Fig. 2, scanning electron micrography was employed to illustrate the difference in surface morphology of the raw synthetic graphite (MCMB) and the metal-coated graphites (samples S1–S3). Fig. 2a gives the surface morphology of raw MCMB. A quite smooth surface with very few pores is observed. Particles of sample S1 are uniformly distributed throughout the speciemen, as seen in Fig. 2b. For sample S2 (Fig. 2c), smaller particles are deposited compared with sample S1. It can also be noticed that the surface coverage by tin-oxide particles is lower in sample S1 than is sample S2. This difference is caused by the different reaction times when preparing samples S1 and S2. The reaction time for sample S1 was 30 min and that for sample S2 was 10 min at the same temperature of 500 °C (see Table 1). The longer reaction time provides more of the source and sufficient surface diffusion time for grain growth. The surface morphology of two coated layers is shown in Fig. 2d. Two distinctive layers can be recognised: the larger and brighter particles are copper, and the smaller and darker particles underneath are tin-oxide particles. The particles of the tin-oxide are about 50 nm in diameter and have a spherical shape, and those of copper are about 200 nm in diameter also with a spherical shape. The surface coverage patterns of copper and tin-oxide are relatively uniform.

The X-ray diffraction patterns of raw graphite, graphite coated with tin-oxide and the graphite coated with tin-oxide and copper by FCVD are shown in Fig. 3. The typical peak of hexagonal structure in graphite and the characteristic diffraction peaks of SnO_2 (JCPDS 41-1445) and copper (JPCDS 04-0836) are observed. The peak intensities of the tin-oxides become stronger with reaction time, and there determine the amount of metal deposited on the graphite surface.

Fig. 4 shows the first and second charge–discharge curves for raw synthetic graphite and metal-coated graphites with different contents, i.e. 0.93 wt.% (S1), 1.37 wt.% (S2) and 1.83 wt.% (S3). The electrolyte was 1 M $LiPF_6$ in EC:EMC:DEC (1:1:1). Although the curves for S1 and

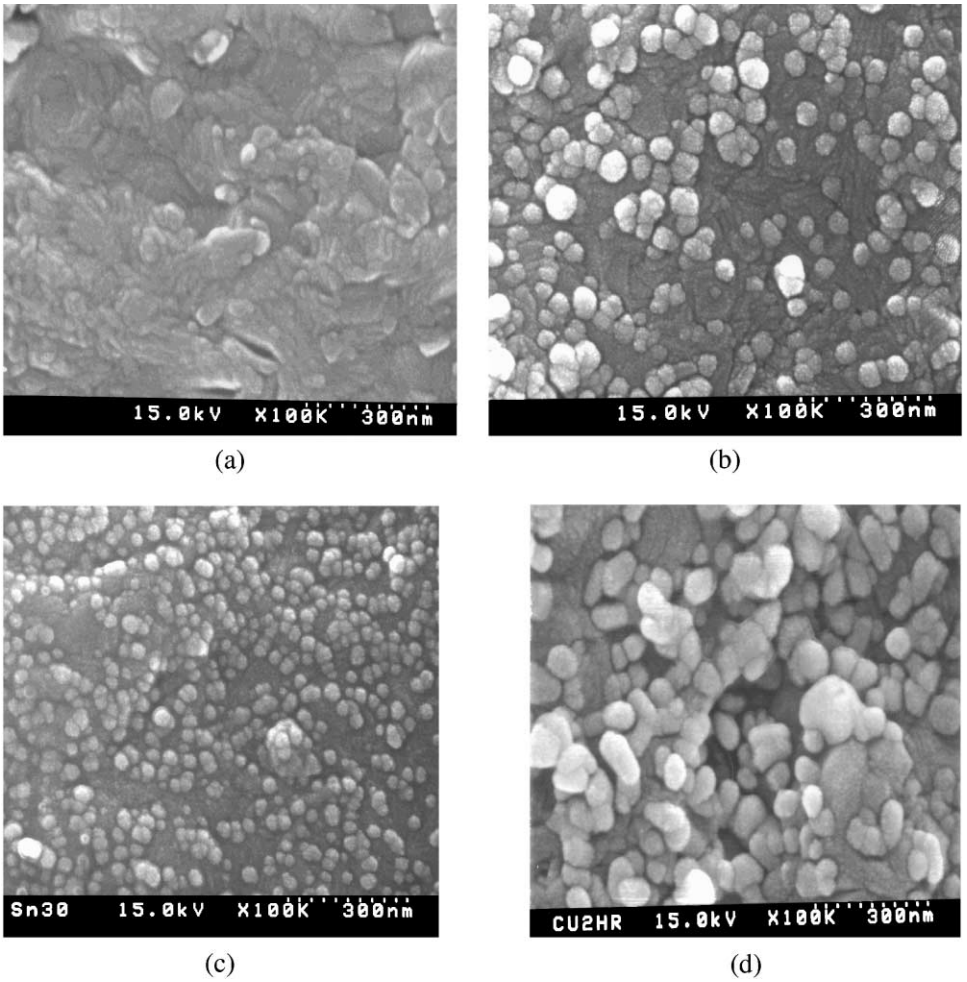

Fig. 2. Scanning electron micrography of metal-coated graphites: (a) S0; (b) S1; (c) S2; (d) S3.

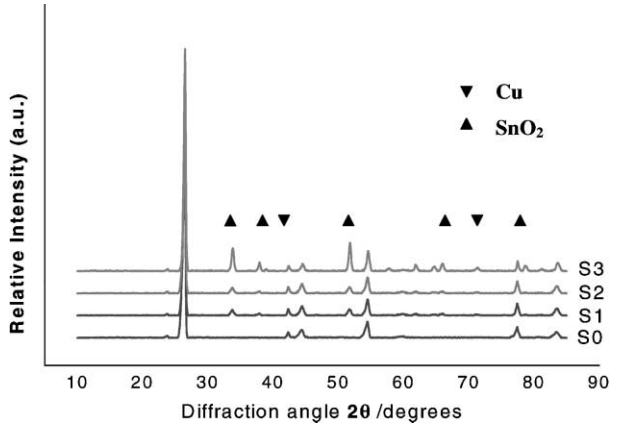

Fig. 3. X-ray diffraction patterns of raw graphite and metal-coated graphites.

S2 have a similar form compared with that for graphite (S0), an irreversible reaction is observed at near 0.7 V versus Li^+/Li for S3. As shown, an excess charge consumption during the first cycle was observed for all the samples due to the formation of a passivation film or the formation of metal–lithium alloy. In the second subsequent cycles, however, the charge consumption for Li^+ intercalation is lower and the charge recovery is close to 100%.

Table 2 lists the specific charge capacities, discharge capacities and initial efficiencies of graphite (S0) and metal-coated graphites (S1, S2, S3) in electrolytes of various composition. The values of these parameters are dependent on the composition of the electrolyte. The specific charge capacities and discharge capacities of metal-coated graphites are larger than that of the raw graphite anode, S0. For the tin-oxide coated graphite anodes, the specific charge capacities and discharge capacities increase, while the initial efficiencies decrease with increase in the weight of tin-oxide which is deposited.

According to the results of Courtney and Dahn [10], lithium bonds oxygen from the tin-oxide structure during first charging cycle, and tin metal and Li_2O are formed by break up of the oxides as follows:

$$SnO_2 + 2Li \rightarrow SnO + Li_2O \quad (1)$$

$$SnO + 2Li \rightarrow Sn + Li_2O \quad (2)$$

The reactions can be confirmed by characterisation of the SnO_2-coated graphite anode. As shown in Fig. 5, scanning electron micrography was employed to explain the

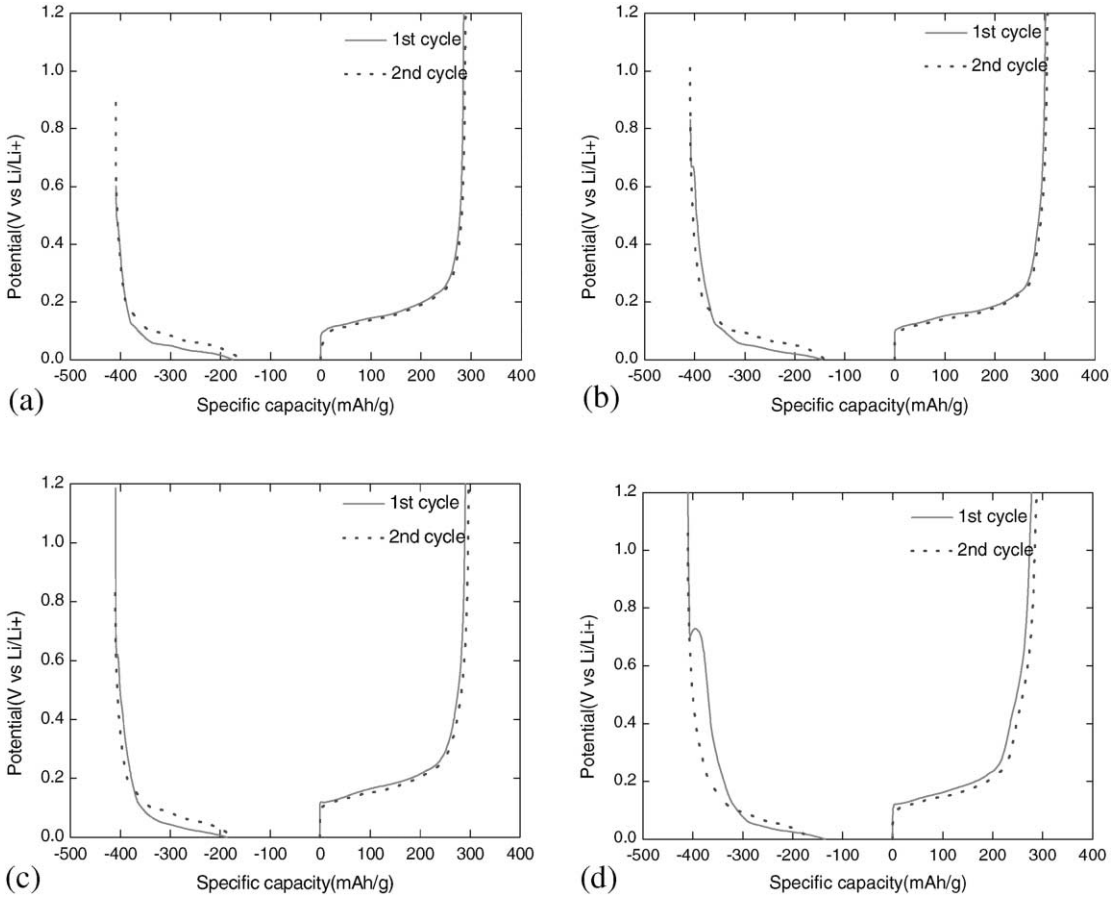

Fig. 4. First and second charge–discharge curves of raw graphite and metal-coated graphites (1 M $LiPF_6$ in EC:EMC:DEC (1:1:1) electrolytes at C/5: (a) S0; (b) S1; (c) S2; (d) S3).

Table 2
First charge–discharge cycle capacities and initial efficiencies of graphite and metal-coated graphite for various composition of electrolyte

Electrolyte[a]	S0			S1			S2			S3		
	CC[b]	DC[c]	IE[d]	CC[b]	DC[c]	IE[d]	CC[b]	DC[c]	IF[d]	CC[b]	DC[c]	IE[d]
EC:EMC:DMC (1:1:1)	297	271	91	324	289	89	329	292	89	361	283	78
EC:EMC:DEC (1:1:1)	314	285	91	334	297	89	326	291	89	365	288	79
EC:DEC (1:2)	314	286	91	327	291	89	337	301	89	365	282	77
EC:EMC (1:2)	302	277	92	333	297	89	322	288	89	358	280	78

[a] Li salt of 1 M $LiPF_6$.
[b] CC: charge capacity (mAh^{-1} g).
[c] DC: discharge capacity (mAh^{-1} g).
[d] IE: initial efficiency (%).

difference in surface morphology between the electrode with tin-oxide and another electrode after 30 charge–discharge cycles. Fig. 5a shows the surface morphology of tin-oxide to have very few pores, while a rather rough surface and pores were observed after 30 cycles, see Fig. 5b. This suggests that the oxygen atoms in tin-oxide react with lithium to form tin during cycling. The XRD spectra of tin-oxide-coated graphite and an electrode after 30 cycles are compared in Fig. 6. As shown, the tin-oxide peaks disappear after cycling, while the reduced tin peaks appeared.

The discharge capacity of the various samples prepared by fluidised-bed CVD and for the synthetic graphite are compared in Fig. 7. The tin-oxide-coated MCMB, S1 gave higher discharge capacity than that of the raw graphite on

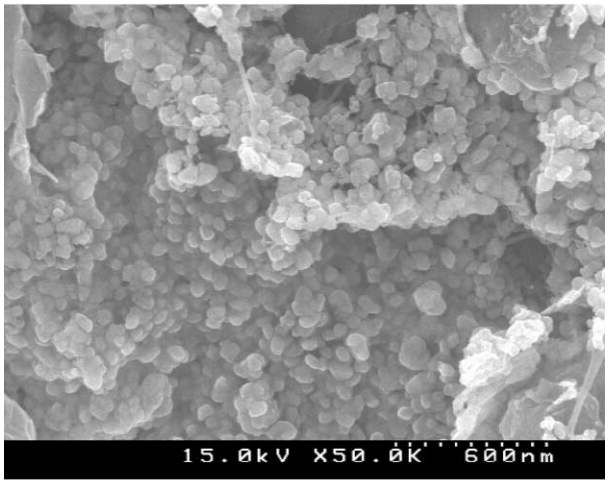

Fig. 5. Scanning electron micrographs of tin-oxide coated carbon: (a) before charge–discharge; (b) after 30 cycles.

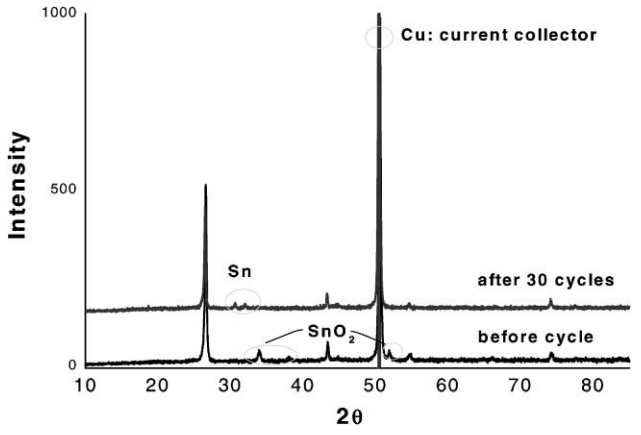

Fig. 6. X-ray diffraction patterns of tin-oxide coated electrodes before and after cycling.

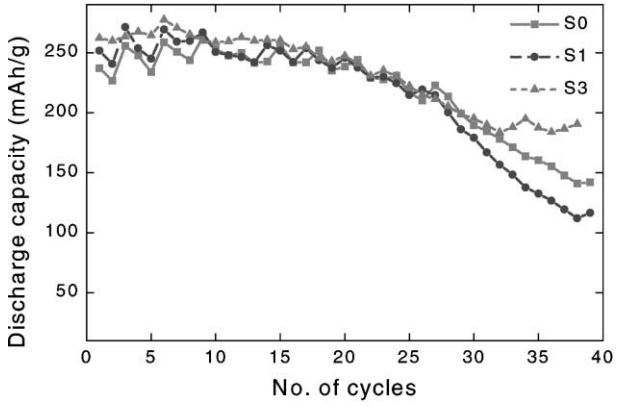

Fig. 7. Comparison of cycling performance of electrodes made from S0, S1, S3 (1 M $LiPF_6$ in EC:EMC:DMC (1:1:1)).

initial cycles, but the capacity clearly decreases after 10 cycles. The behaviour of sample S2 was very similar to that of S1. By contrasts, the copper–tin-oxide coated sample, S3, maintained a higher performance with cycling. This is possibly due to the buffering effect of copper against severe volume changes of tin-oxide.

Evidence for the presence of passivation film formation can be found in Fig. 8. In Fig. 8a, no peaks were observed over the range 0.6–0.8 V versus Li/Li^+, both in the first and the second cycles. As shown in Fig. 8b and c, however, passivation peaks due to the interfacial reaction between the metals (tin-oxide and copper) and the electrolyte are clearly

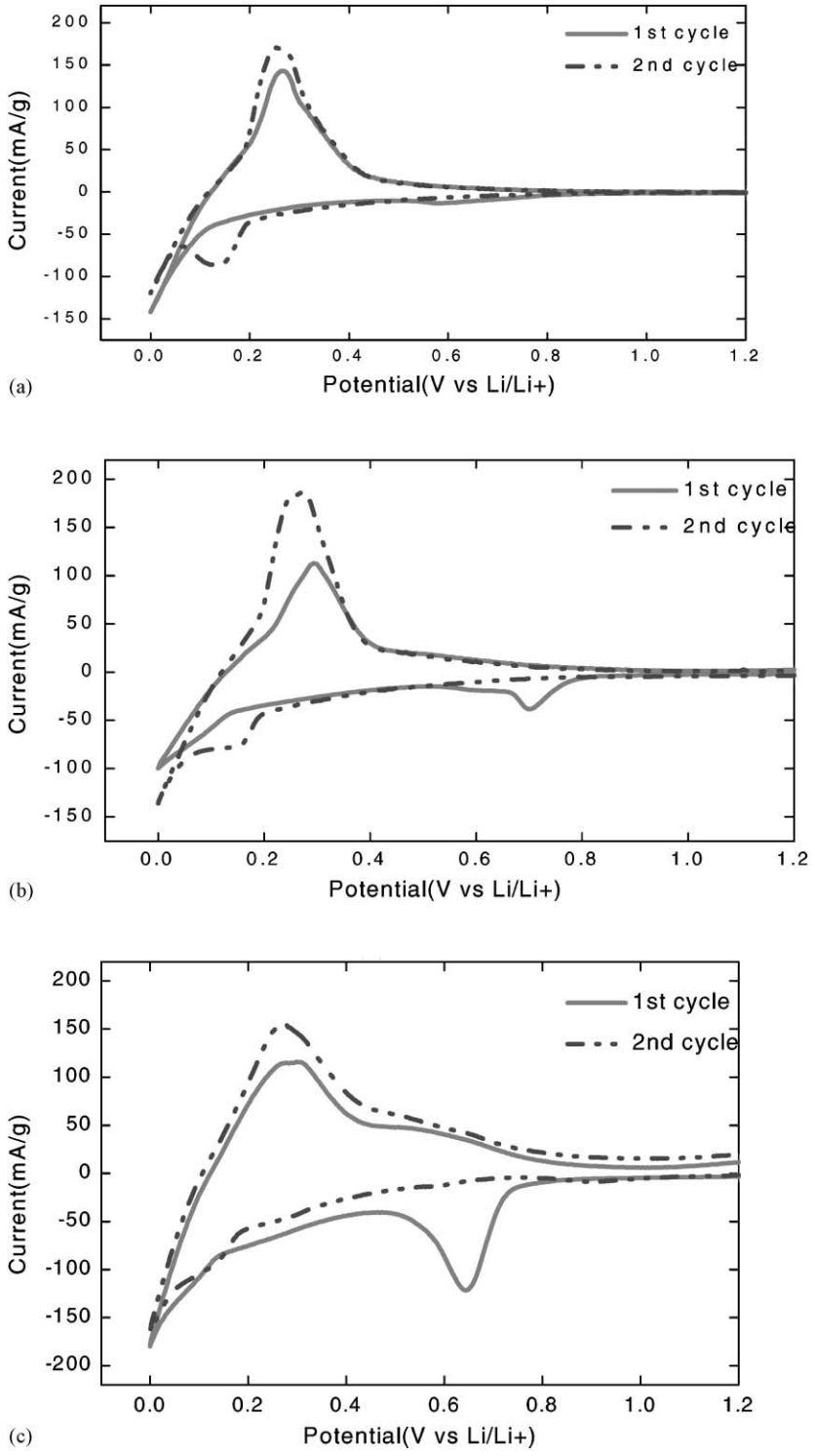

Fig. 8. Cyclic voltammograms at scan rate of 0.1 mV^{-1} s (0.0 ↔ 3.0 V): (a) S0; (b) S1; (c) S3.

present. The much stronger peak for S3 means that the copper is more easily passivated than tin-oxide, which may lead the better electrochemical performance.

A family of Nyquist plots measured for S0, S1, S2, S3 cells during the course of Li intercalation and de-intercalation in different liquid electrolytes with various compositions is given in Fig. 9. For all samples, semi-circles appear and the equivalent circuit comprises an electrolytic resistance and an interfacial resistance. The inserts represent the EVS and the numbers in the EVS indicate the point of potential range at which the ac impedance was measured. The diameters of the slightly depressed semicircles represent the charge-transfer resistance from electrochemical reactions. It is observed that the diameter of the semicircle for S0 at 0.06 V versus Li/Li$^+$ (indicated as 3 and (▲) in Fig. 9a is the largest, which indicates that no sites remained within the graphite layer to intercalate with lithium. The semicircle of S0 at 0.8 V versus Li/Li$^+$ (indicated as 1 and (■) in Fig. 9a is not clearly seen, while the other electrodes from S1, S2 and S3 obviously show semicircles at 0.8 V versus Li/Li$^+$ (indicated as 1 and (■) in Fig. 9b–d, which results from the alloy reaction between lithium and tin-oxide. It is also seen that the diameter of the semicircle, i.e. the faradic impedance of the electrode, decreases sharply with increase in tin-oxide content. S3 has a slightly larger impedance than that of S1 in spite of the greater amount of tin-oxide in S3. A feasible explanation can be made by considering the addition of inactive copper matrix in the tin-oxide coating of S3. It can be concluded that addition of copper improves the cycleability of the electrode, but reactivity decreases.

The discharge capacities at three different rates with various electrolyte compositions are shown in Table 3. The table shows that the discharge capacity increases with the amount of tin-oxide due to the lithium alloying reaction with tin-oxide. The change in the capacity at various rates when 1 M $LiPF_6$ in EC:EMC:DMC (1:1:1) electrolyte is used is shown in Fig. 10. The discharge capacities of the

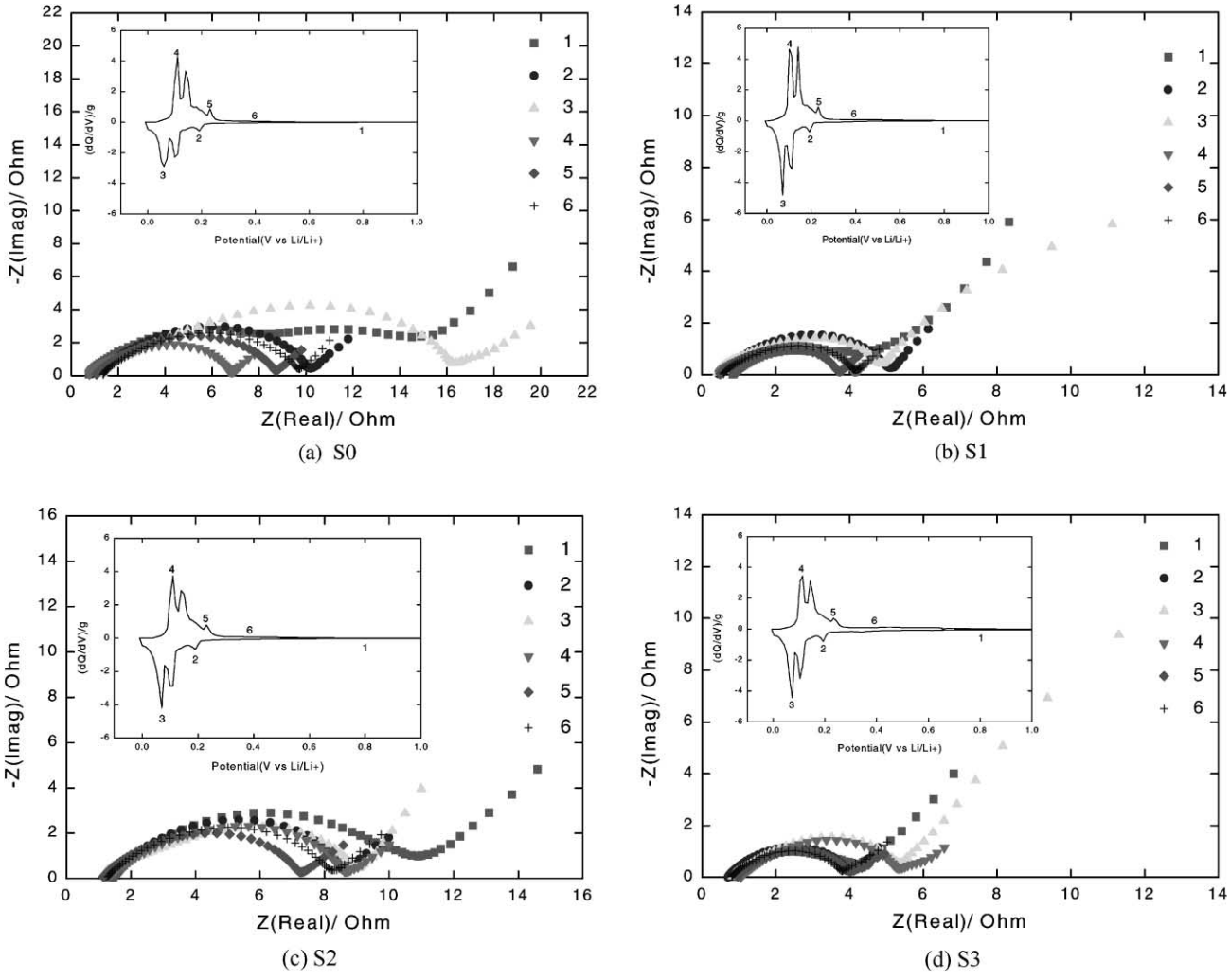

Fig. 9. Nyquist plots measured at second cycle of intercalation and de-intercalation (1 M $LiPF_6$ in EC:EMC:DMC (1:1:1)). Inserts represent electrochmical voltage spectroscopy (EVS). Numbers in EVS indicate points of potential voltage range at which ac impedance is measured (1 and (■): 0.8 V vs. Li/Li$^+$, 2 and (●): 0.17 V vs. Li/Li$^+$, 3 and (▲): 0.06 V vs. Li/Li$^+$, 4 and (▼): 0.13 V vs. Li/Li$^+$, 5 and (◆): 0.22 V vs. Li/Li$^+$, 6 and (+): 0.4 V vs. Li/Li$^+$).

Table 3
Discharge capacities of graphite and the metal-coated graphites of various compositions of electrolyte and different C rates

Electrolyte	S0			S1			S2			S3		
	C/5	C/3	C/2	C/5	C/3	C/2	C/5	C/3	C/2	C/5	C/3	C/2
EC:EMC:DMC (1:1:1)	288	281	268	302	282	268	305	305	284	310	291	269
EC:EMC:DEC (1:1:1)	290	280	265	304	284	267	298	298	277	305	285	270
EC:DEC (1:2)	295	277	263	302	285	266	302	302	282	325	284	265
EC:EMC (1:2)	290	285	266	302	291	273	299	299	285	308	297	272

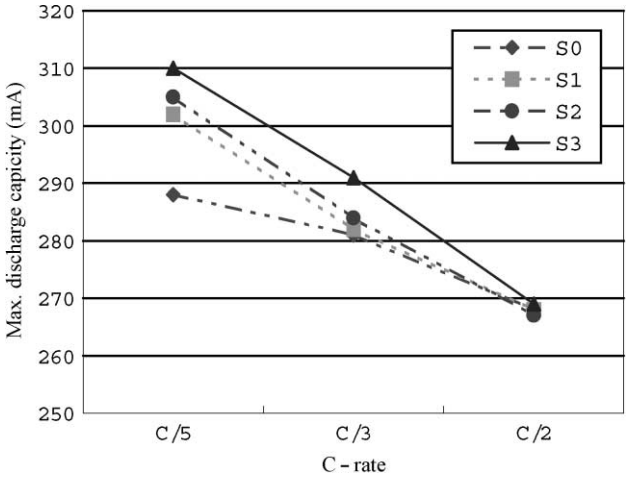

Fig. 10. Effect of tin-oxide and copper coating on maximum discharge capacity at various C rates. 1 M $LiPF_6$ in EC:EMC:DMC (1:1:1).

metals-coated graphites S1, S2 and S3 are higher than that of S0 at the C/5 rate. Regardless of the amount of coating, however, the discharge capacities of all test species decrease with increase in charge–discharge rate and become almost the same at the C/2 rate. The change in pattern with C rate can be explained by considering the factors that influence the electrochemical performance. The major factors are the transfer of lithium ions and the lithium alloying reaction during cycling.

The lithium alloying reaction with tin-oxide at relatively low C rates leads to an increase in discharge capacity. On the other hand, the lithium alloying reaction at higher C rates does not proceed because the lithium deintercalation rate is too fast to react with tin-oxide. Therefore, the effect of tin-oxide coating is insignificant at high C rates.

4. Conclusion

Synthetic graphite, MCMB, has been coated with tin-oxide and copper by the fluidised-bed chemical vapour deposition (CVD) method and the coating effect on electrochemical characteristics has been investigated. Spherical shaped tin-oxide of about 50 nm diameter and copper of about 200 nm diameter deposited on the graphite surface can be observed after fluidised CVD experiment. Three different metal-coated graphites and raw MCMB have been used as lithium secondary battery anodes to investigate their coating effects on electrochemical characteristics.

The electrodes prepared with tin-oxide coated graphite give higher capacity than the raw material. The impedance of the surface film decreases as the content of tin-oxide is increased, and this results in higher capacity. The capacity decreases, however, with cycling, which could be due to severe volume changes of the tin-oxide during cycles. The cycleability of the electrode is improved by coating copper on the surface carbon coated with tin-oxide. This plays an important role as an inactive matrix which buffers against the volume changes. The effect of the tin-oxide coating is insignificant at high C rates because the relative lithium deintercalation rate is too fast to cause an alloying reaction between the lithium and the tin-oxide.

It is concluded that, fluidised-bed CVD developed in the present study is an effective method to modify the active electrode materials of lithium secondary batteries.

References

[1] Z.X. Shu, R.S. McMillan, J.J. Murray, J. Electrochem. Soc. 140 (1993) L101.
[2] K. Ikawa, M. Nanba, M. Mizumoto, S. Nishimura, K. Tamura, Denki Kogaku 59 (1991) 891 (in Japanese).
[3] K. Nishimura, H. Honbo, M. Mizumoto, T. Horiba, in: Proceedings of the 7th International Meeting on Lithium Batteries, Ext. Abstract, Boston, WA, USA, 15–20 May 1994, pp. 232–234.
[4] J. Aragane, K. Matsui, H. Andoh, S. Suzuki, H. Fukuda, H. Ikeya, K. Kitaba, R. Ishikawa, J. Power Sources 68 (1997) 13–18.
[5] H. Momose, H. Honbo, S. Takeuchi, K. Nishimura, T. Horiba, Y. Muranaka, H. Miyadera, Y. Kozono, J. Power Sources 68 (1997) 208–211.
[6] K. Nishimura, H. Honbo, S. Takeuchi, T. Horiba, M. Oda, M. Koseki, Y. Muranaka, Y. Kozono, H. Miyadera, J. Power Sources 68 (1997) 436–439.
[7] T.H. Kang, B.W. Cho, W.I. Cho, J.B. Ju, K.S. Yun, in: Proceedings of the 196th Meeting of the Electrochemical Society, Abstract No. 307, Hawaii, USA, 17–22 October 1999.
[8] T.H. Kang, J.K. Lee, B.W. Cho, W.I. Cho, J.B. Ju, K.S. Yun, Electrode properties of tin-oxide-coated graphite as a negative electrode for lithium secondary batteries, in: Proceedings of the 1st World Conference on Carbon (Eurocarbon 2000), Berlin, Germany, 9–13 July 2000, pp. 841–842.
[9] N. Takami, A. Satoh, M. Hara, T. Ohasaki, J. Electrochem. Soc. 142 (1995) 371.
[10] I.A. Courtney, J.R. Dahn, Electrochem. Soc. 144 (1997) 2045.